Available online at www.sciencedirect.com

ScienceDirect

Physics Engineering 10 (2011) 3026–3031

Engineering Procedia

11th International Conference on the Mechanical Behavior of Materials

In-plane elastic properties of hierarchical cellular solids

Nicola M. Pugno[a]*, Qiang Chen[a]

[a]Laboratory of Bio-Inspired Nanomechanics "Giuseppe Maria Pugno",Department of Structural Engineering and Geotechnics, Politecnico di Torino, Torino, 10129, Italy.

Abstract

In this paper, we analytically calculate the in-plane linear-elastic properties of a new class of bio-inspired nano-honeycomb materials possessing a hierarchical architecture, which is often observed in natural materials. Incorporating the surface tension, peculiar of the nano-scale, modifications of the classical results for macroscopic and nonhierarchical honeycombs are proposed. A parametrical analysis reveals the influences of relative density and of two key geometrical parameters on the overall elastic properties. We discover optimal values for some of the mechanical properties, e.g. stiffness-to-density ratio. The developed theory allows us to design a new class of materials with tailored elastic properties at each hierarchical level and could be useful for many applications.

Keywords: Hierarchical; Nano-honeycomb; Orthotropic Material; Elastic constants.

1. Introduction

Honeycomb materials, due to their special structures and properties, are very promising for structural, mechanical and material design, e.g. they are used as a core material in sandwich structures for energy absorption [1]. One of the important issues in material science is to characterize and model the in-plane and out-plane mechanical behaviors [2-5] of honeycomb structures. For the in-plane deformation mechanism, the stress-strain curve [3-6] is described by three regimes (the linear elastic, plateau and densification regions). If the honeycomb structure is nano-sized, the surface effect should be taken into account because of the high surface-to-volume ratio. Extensive works [7-11] studied the influence of the

* Corresponding author. Tel.: +39-011 564 4902; fax: +39-011 564 4899.
E-mail address: nicola.pugno@polito.it.

1877–7058 © 2011 Published by Elsevier Ltd.
doi:10.1016/j.proeng.2011.04.501

surface effect on the linear elastic behaviors of nanowires, since nano-wires or nano-rods hold a promise for nano-device applications.

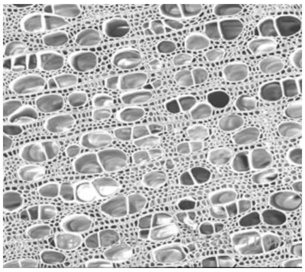

Fig. 1 SEM image of pure aspen wood [15].

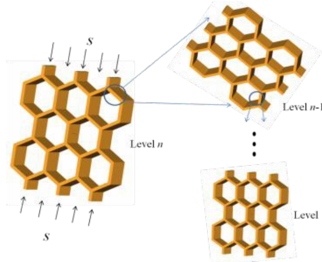

Fig. 2 Hierarchical nano-honeycombs.

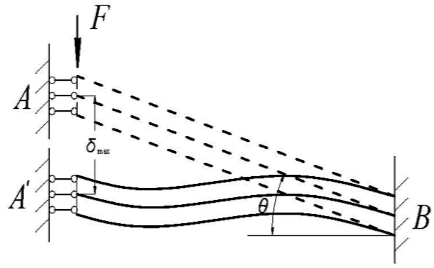

Fig. 3 An inclined orthotropic beam.

In this paper, we construct a hierarchical nano-honeycomb structure [12-14], inspired by biological materials (Fig. 1) [15], and study its in-plane elastic properties (Fig. 2). Here, starting from an orthotropic constituent material and considering the influence of the surface effect, we derived the effective longitudinal Young's modulus of the *n*-level structure thanks to a classical iterative approach [16]. Besides, we also find the expressions for the stiffness-to-density ratios. Finally, we perform a parametric analysis to investigate the influences of the relative density and the geometrical parameters on the overall elastic behaviors.

2. Deflection of an orthotropic beam with surface effect

Assuming the conservation of plane sections, for the elastic line of an orthotropic beam with principal direction 1 coincident with the beam axis (Fig. 3). The classical expression for the deflection of the Euler beam is found [6,17,18]:

$$\delta_{\max} = \frac{Fl^3}{12E_1 I}\cos^2\theta \tag{1}$$

where, $\delta_{\max}$ is the vertical displacement of the guided end of the orthotropic beam, F is the concentrated force acting on the guided end, l is the beam length, $E_1 I$ is the flexural rigidity, and θ is the inclined angle between beam and horizontal line.

If the beam is nano-sized, the modification of the influence of the surface effect should be considered, finding the maximum displacement as [9]:

$$\delta_{\max} = \frac{Fl^3}{12\left(E_1 I\right)^{eq}}\cos^2\theta \tag{2}$$

with

$$\left(E_1 I\right)^{eq} = \frac{1}{12}E_1 bt^3 + \frac{1}{2}E_s bt^2 + \frac{1}{6}E_s t^3 \tag{3}$$

where, $\left(E_1 I\right)^{eq}$ is the equivalent flexural rigidity; *b*, *t* are width and thickness of the beam, respectively; E_s, which depends on the crystal orientation [19], is the surface Young's modulus.

3. Linear-elastic properties of hierarchical nano-honeycombs

3.1. Elastic constants of hierarchical nano-honeycombs

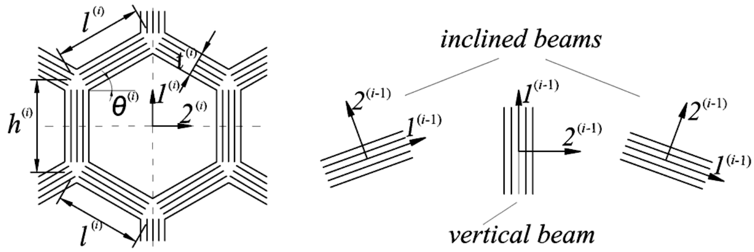

Fig. 4 Schematic of the honeycomb at level *i*.

Fig. 4 describes the *i*-level of the nano-honeycomb. The structure at level *i* is constructed basing on the structure at level *i*-1. The deformation is caused by the bending of the inclined cell-walls and the compression of the vertical cell-walls, namely, the beam along which the force is applied, but the compressive deformation is neglected with respect to the bending deflection. Thus, basing on eqns. (1)-(3) and employing the classical method [6] and an iterative process [16], we find the elastic constants of the hierarchical honeycomb.

For the longitudinal Young's modulus, we find:

$$\frac{E_1^{(n)}}{E_1^{(0)}} = \prod_{i=1}^{n} \lambda_s^{(i)} f_1^{(i)} f_4^{(i)} \cdot \left(\frac{\rho^{(n)}}{\rho^{(0)}}\right)^3 \tag{4}$$

whereas the transverse Young's modulus and shear modulus are:

$$\begin{aligned} \frac{E_2^{(n)}}{E_1^{(0)}} &= \frac{f_2^{(n)}}{f_1^{(n)}} \cdot \frac{E_1^{(n)}}{E_1^{(0)}} \\ \frac{G_{12}^{(n)}}{E_1^{(0)}} &= \frac{f_3^{(n)}}{f_1^{(n)}} \cdot \frac{E_1^{(n)}}{E_1^{(0)}} \end{aligned} \tag{5}$$

The Poisson's ratios are:

$$\mu_{12}^{(n)} = \left(\frac{f_1^{(n)}}{f_2^{(n)}}\right)^{0.5} = \frac{1}{\mu_{21}^{(n)}} \tag{6}$$

with

$$\begin{aligned} f_1^{(i)} &= \frac{(h^{(i)}/l^{(i)} + \sin\theta^{(i)})}{\cos^3\theta^{(i)}} \\ f_2^{(i)} &= \frac{\cos\theta^{(i)}}{(h^{(i)}/l^{(i)} + \sin\theta^{(i)})\sin^2\theta^{(i)}} \\ f_3^{(i)} &= \frac{(h^{(i)}/l^{(i)} + \sin\theta^{(i)})}{(h^{(i)}/l^{(i)})^2(1 + 2h^{(i)}/l^{(i)})\cos\theta^{(i)}} \\ f_4^{(i)} &= \left(\frac{2\cos\theta^{(i)}(h^{(i)}/l^{(i)} + \sin\theta^{(i)})}{(h^{(i)}/l^{(i)} + 2)}\right)^3 \end{aligned} \tag{7}$$

$$\lambda_s^{(i)} = 1 + 2\frac{E_s^{(i-1)}}{E_1^{(i-1)} t^{(i)}}\left(3 + \frac{t^{(i)}}{b}\right) \tag{8}$$

where, $E_1^{(i-1)}$ and $E_s^{(i-1)}$ are the bulk and surface Young's moduli in the principal direction $1^{(i-1)}$ (zero*th* level), respectively; b and $t^{(i)}$ are width and thickness of cross-sections of cell walls, respectively; $l^{(i)}$

and $h^{(i)}$ are lengths of inclined and vertical beams, respectively; $\theta^{(i)}$ is the included angle made by the inclined beam and the horizontal line (Fig. 4).

Note that, the reciprocal theorem holds:

$$E_1^{(n)}\mu_{21}^{(n)} = E_2^{(n)}\mu_{12}^{(n)} \tag{9}$$

Eqns. (4)-(6) show that the transverse Young's modulus and shear modulus can be derived from the longitudinal Young's modulus, and two Poisson's ratios are only related to the geometry of the *n*-level structure.

From eqns. (8), we note that the Young's moduli and shear modulus are modified by a factor $\lambda_s^{(i)}$. If $t_1^{(i)}/b \ll 3$ (i.e. plate), eqn. (8) can be expressed as:

$$\lambda_s^{(i)} = 1 + 6\frac{E_s^{(i-1)}}{E_1^{(i-1)}t^{(i)}} \tag{10}$$

Expression (9) coincides with the result from [20], and it obeys the scaling law $\lambda_s^{(i)} = 1 + \alpha l_{\text{in}}/t^{(i)}$ [21] with $l_{\text{in}} = E_s^{(0)}/E_1^{(0)}$ and $\alpha = 6.0$. Note that, l_{in} is a material intrinsic length, under which surface effect plays an important role compared to bulk; α is a dimensionless constant, which depends on the geometry of the structural elements and their deformations. Besides, we can see that the surface effect makes the structure stiffer if $E_s^{(i)} > 0$; otherwise, it makes the structure softer.

3.2. The stiffness-to-density ratio

The stiffness-to-density ratio can be derived easily basing on eqns. (4) and (5), i.e.

$$\frac{E_1^{(n)}}{\rho^{(n)}} = \frac{E_1^{(0)}}{\rho^{(0)}}\prod_{i=1}^{n}\lambda_s^{(i)}f_1^{(i)}f_4^{(i)}\cdot\left(\frac{\rho^{(n)}}{\rho^{(0)}}\right)^2 \tag{11}$$

$$\frac{E_2^{(n)}}{\rho^{(n)}} = \frac{f_2^{(n)}}{f_1^{(n)}}\cdot\frac{E_1^{(n)}}{\rho^{(0)}}$$
$$\frac{G_{12}^{(n)}}{\rho^{(n)}} = \frac{f_3^{(n)}}{f_1^{(n)}}\cdot\frac{E_1^{(n)}}{\rho^{(0)}} \tag{12}$$

4. Parametric analysis and discussion

Here, we use silver (Ag) as the constituent material and a five-level hierarchical nano-honeycomb structure. The Young's modulus and density of Ag are 78GPa and 10.94g/cm^3, respectively; the surface elastic modulus is $E_s = 1.22\text{N/m}$ on the (001) surface A [11]; the thickness of the cell walls at the first level is $t^{(1)} = 5\text{nm}$.

For the reasons that we discussed in section 3, only $E_1^{(n)}$ is treated here. First, we investigated the influence of the relative density (0.2, 0.3, 0.4). Second, under the condition of $\rho^{(i+1)}/\rho^{(i)} = 0.3$, the influences of $h^{(i)}/l^{(i)}$ and $\theta^{(i)}$ are studied. The analytic results of the longitudinal Young's modulus and the stiffness-to-density ratio are reported in Fig. 5 and Fig. 6, respectively. They show that the longitudinal Young's modulus increases as $\rho^{(i+1)}/\rho^{(i)}$, $h^{(i)}/l^{(i)}$ or $\theta^{(i)}$ increase, but decreases as level *n* increases: there is no any maximum value (Fig. 5(a), Fig. 6(a) and (b)); in contrary, the stiffness-to-density ratio has an optimal value at level 2 for $\rho^{(i+1)}/\rho^{(i)} = 0.4$ (Fig. 5(b)) and at level 3 with the variation of $h^{(i)}/l^{(i)}$ (Fig. 6(c)). Fig. 6(d) implies that stiffness-to-density can also reach a maximum value with the increase of $\theta^{(i)}$.

Fig. 5 and Fig. 6 indicate that the elastic behaviour can be tuned by changing the relative density and geometric configuration. Increasing $\theta^{(i)}$ or $h^{(i)}/l^{(i)}$ the Young's modulus increases. The reason is

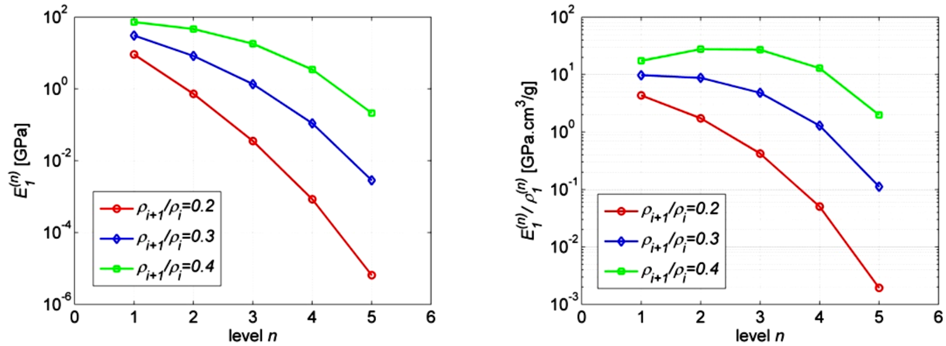

(a) (b)

Fig. 5 Longitudinal Young's modulus and stiffness-to-density ratio vs level *n*. (a) Influence of the relative density on the stiffness; (b) Influence of the relative density on the stiffness-to-density ratio

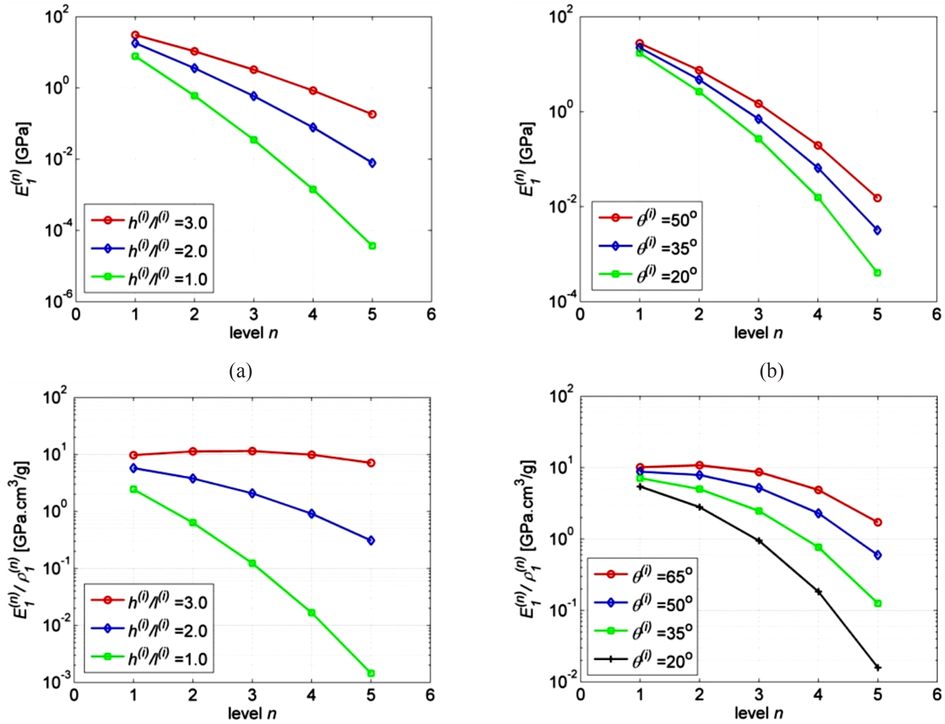

(a) (b) (c) (d)

Fig. 6 Longitudinal Young's modulus and stiffness-to-density ratio vs level *n*. (a) Influence of $h^{(i)}/l^{(i)}$ on longitudinal Young's modulus (for each $h^{(i)}/l^{(i)}$, $\theta^{(i)}=70-10i$); (b) Influence of $\theta^{(i)}$ on longitudinal Young's modulus (for each $\theta^{(i)}$, $h^{(i)}/l^{(i)}=3.5-0.5i$); (c) Influence of $h^{(i)}/l^{(i)}$ on stiffness-to-density ratio (for each $h^{(i)}/l^{(i)}$, $\theta^{(i)}=70-10i$); (d) Influence of $\theta^{(i)}$ on stiffness-to-density ratio (for each $\theta^{(i)}$, $h^{(i)}/l^{(i)}=3.5-0.5i$).

that their increases lead to the reduction of strain and under the same external force, the stiffness increases. If $\theta^{(i)}$ (or $h^{(i)}/l^{(i)}$) increases, while $h^{(i)}/l^{(i)}$ (or $\theta^{(i)}$) decreases, then, the two variations of $\theta^{(i)}$ or $h^{(i)}/l^{(i)}$ result in an inverse tendency (i.e., the former makes the Young's modulus larger; the latter makes the

Young's modulus smaller) about the elastic parameters, so, there exist optimal values (Fig. 6 (c)). This finding suggests next strategies towards the design of super-stiff cellular solids.

5. Conclusion

We have calculated the in-plane elastic properties of hierarchical nano-honeycombs. The surface effect modifies the classical results of non-hierarchical honeycomb and it can stiffen or soften the elastic properties of the structures. Employing an iterative process, we derived the stiffness and stiffness-to-density ratio at level *n*. The parametric analysis reveals the influences of the relative density and of two key important parameters on the stiffness and stiffness-to-density ratio, and it shows that the elastic properties can be optimized by tuning these parameters. The present theory may have many interesting applications.

References

[1] Foo CC., Chai GB, Seah LK. Mechanical properties of Nomex material and Nomex honeycomb structure. *Compos Struct* 2007; **80**; 588-594.

[2] Gibson LJ, Ashby MF. The Mechanics of Two-Dimensional Cellular Materials. *Proc R Soc Lond* A 1982; **382**; 25-42.

[3] Papka SD, Kyriakides S. In-plane compressive response and crushing of honeycombs. *J Mech Phys Solids* 1994; **42**; 1499-1532.

[4] Papka SD, Kyriakides S. In-plane crushing of a polycarbonate honeycomb. *Int J Solids Structures* 1998a; **35**; 239-267.

[5] Papka SD, Kyriakides S. Experiments and full-scale numerical simulations of in-plane crushing of a honeycomb. *Acta Mater* 1998b; **46**; 2765-2776.

[6] Gibson LJ, Ashby MF. *Cellular solids: structure and properties,* 2nd ed. Cambridge: Cambridge Universiry Press; 1997.

[7] Cammarata RC. Surface and interface stress effect in thin films. *Prog Surf Sci* 1994; **46**; 1-38.

[8] Gurtin ME, Murdoch AI. A continuum theory of elastic material surface. *Arch Rat Mech Anal* 1975; **57**; 291-323.

[9] Wang GF, Feng XQ. Surface effects on buckling of nanowires under uniaxial compression. *Appl Phys Lett* 2009; **94**; 141913.

[10] Shankar MR, King AH. How surface stresses lead to size-dependent mechanics of tensile deformation in nanowires. *Appl Phys Lett* 2007; **90**; 141907

[11] Wong EW, Sheehan PE, Lieber CM. Nanobeam mechanics: elasticity, strength and toughness of nanorods and nanotubes. *Science* 1997; **277**; 1972-1975.

[12] Pugno NM. Mimicking nacre with super-nanotubes for producing optimized super-composites. *Nanotechnol* 2006; **17**; 5480-5484.

[13] Pugno NM, Bosia F, Carpinteri A. Multiscale stochastic simulations for tensile testing of nanotube-based macroscopic cables. *Small* 2008; **4**; 1044-1052.

[14] Wang XS, Xia R. Size-dependent effective modulus of hierarchical nanoporous foams. *Europhys Lett* 2010; **92**; 16004.

[15] Cai X. Wood modifications for valued-added applications using nanotechnology-based approaches. PhD. Thesis 2007; Université Laval; Canada.

[16] Lakes R. Materials with structural hierarchy. *Nature* 1993; **361**; 511-515.

[17] Tolf G. Saint-Venant Bending of an Orthotropic Beam. *Comp Struct* 1985; **4**; 1-14.

[18] Roark RJ, Young WC. *Formulas for stress and strain*, 5th ed. New York: McGraw-Hill; 1975.

[19] Shenoy VB. Atomistic calculations of elastic properties of metallic fcc crystal surfaces. *Phys Rev* B 2005; **71**; 094104-1.

[20]Miller RE, Shenoy VB. Size-dependent elastic properties of nanosized structural elements. *Nanotechnol* 2000; **11**; 139-147.

[21] Wang J, Duan HL, Huang ZP, Karihaloo BL. A scaling law for properties of nano-structured materials. *Proc R Soc* A 2006; **462**; 1355-1363.